Vol. 730: 95–111, 2024
https://doi.org/10.3354/meps14534

MARINE ECOLOGY PROGRESS SERIES
Mar Ecol Prog Ser

Published March 7

Trace elemental and stable isotopic signatures to reconstruct the large-scale environmental connectivity of fish populations

Zhongya Xuan[1,2], Wen-Xiong Wang[1,2,*]

[1]School of Energy and Environment and State Key Laboratory of Marine Pollution, City University of Hong Kong, Kowloon, Hong Kong, PR China

[2]Research Centre for the Oceans and Human Health, City University of Hong Kong Shenzhen Research Institute, Shenzhen 518057, PR China

ABSTRACT: Animal movements and connectivity across different environments constitute essential components of virtually all ecological and evolutionary processes. In the present study, we measured multiple trace-element profiles and stable isotopes to reconstruct life cycle patterns of *Eleutheronema rhadinum*, and patterns of connectivity among populations of *E. rhadinum* across 3 distinct ecoregions in the eastern China Sea. Our results indicated that *E. rhadinum* larvae from different regions exhibited distinct otolith core levels of trace elements and stable isotopes, serving as discriminative markers of geographical origin. We used the maximum likelihood approach and linear discriminant analysis to trace back the origins of the mixed adult fish stocks. After leaving their nursery areas, juvenile fish from colder northern regions migrated south to overwinter in the South China Sea, where they mixed with the local populations. After overwintering, the adult fish began their long journey north, with the migrating population including individuals of both East China Sea and South China Sea origins. Meanwhile, fish in the Beibu Gulf exhibited a lower degree of interaction with the South China Sea populations and minimal interaction with those in the East China Sea. Trace elements and stable isotopes revealed the spatiotemporal connectivity of *E. rhadinum* across the 3 different ecoregions. This study provides critical information on how marine connectivity supports temperature-mediated fish community movement patterns within coastal ecosystems.

KEY WORDS: *Eleutheronema rhadinum* · Fish movement · Ecoregions · Connectivity · Otolith · Element · Stable isotope

1. INTRODUCTION

Fish exhibit varying requirements at different life stages, such as distinct food resources, predation refugia, suitable water temperature and salinity, and specific habitats to fulfill their reproductive needs (Bradley et al. 2020, Whitfield 2020). These requirements are sometimes difficult to satisfy within a single environment. The movement of animals between various environments during their life cycle influences the resources and spaces they encounter and utilize, and defines their interactions with the surrounding environment (Aykanat et al. 2015, Baerwald et al. 2016, Micheletti et al. 2018, Martín-Vélez et al. 2020). As a result, dispersal to environments with appropriate conditions and necessary resources during different life stages plays a crucial role in maximizing reproductive success and species survival (Burns et al. 2020, Whitfield 2020). Therefore, knowledge of life stage connectivity is important for spatially explicit management of wildlife populations. It can also provide the basis for establishing, expanding, and zoning protected areas for endangered species, and serves as a powerful tool for natural resource management and

*Corresponding author: wx.wang@cityu.edu.hk

conservation (Lowerre-Barbieri et al. 2016, Benson et al. 2019, Burns et al. 2020, Martín-Vélez et al. 2020).

Patterns of migration for some fish include reproductive (or spawning migration), foraging (or feeding migration), and/or overwintering (temperature-adaptive migration) (McDowall 1997). Some species will migrate as juveniles to overwintering areas during seasonal changes in water temperature in search of suitable living conditions and later, as they become reproductively mature, they initiate the next stage of their life cycle by preparing to find suitable spawning grounds (Younes et al. 2020). The pursuit of favorable conditions is an essential driving force in shaping the spatiotemporal distribution of fish species (Alò et al. 2021). Such migration offers the possibility for connectivity among fish populations across disparate regions. This inter-populational connectivity facilitates the genetic exchange among individuals in distinct locations, enhancing the genetic diversity and thereby the resilience and adaptability of populations against extrinsic stressors. The connectivity across various geographical locations promotes the sustainability of fish resources. Understanding population connectivity can therefore guide the formulation of effective fisheries management strategies, such as seasonal fishing moratoriums and catch quotas. Additionally, it enables the establishment of habitat restoration strategies and assists in predicting the ramifications of climate change on fish populations, thereby informing the development of appropriate adaptive measures. Mapping the migration routes is thus crucial for understanding fish behavior, habitat requirements, and population connectivity, and can aid in effective design of management and conservation actions (Burns et al. 2020).

Studying fish movement underwater is challenging because they are difficult to see and track, especially over extensive spatial and/or temporal scales. Otoliths, endogenous structures in the inner ears of teleost fish, offer valuable insights into the movement history and ecological connections of fish species (Ethier et al. 2014, Baker et al. 2019). Otoliths are metabolically inert calcium carbonate deposits that form in chronological order on an organic matrix within the inner ear of bony fish. As fish grow, trace elements are deposited onto the growing otolith surface, some of which are at concentrations that reflect those in the environment (Hüssy et al. 2021). As a result, the chemical variations of otoliths may be used to retrospectively determine the geographic origin and life history changes (Hüssy et al. 2021). Regional variations in water chemistry affect the incorporation of certain elements (mainly Sr and Ba) into otoliths, linking their concentrations in otoliths to those in the surrounding water and enabling the reconstruction of environmental changes experienced throughout the life history of fish (Izzo et al. 2018, Hüssy et al. 2021). In contrast, the carbon isotope ratios ($\delta^{13}C$) in otoliths reflect the dissolved inorganic carbon in environmental water and diet, while otolith $\delta^{18}O$ is primarily controlled by the $\delta^{18}O$ in environmental water and the temperature of the water (Itakura et al. 2018, Kawazu et al. 2020, Sakamoto et al. 2022). Therefore, otolith elemental concentrations and stable isotope values provide natural tags to assess the distribution shifts in fish species at different life stages.

The fourfinger threadfin *Eleutheronema rhadinum* belongs to the family Polynemidae and is distributed along the East Asian coast (Motomura 2004). *E. rhadinum* is a predator in coastal and estuarine ecosystems. Larvae primarily feed on copepods and mysids, with shrimp and prawn larvae also being important prey. Juveniles mainly consume prawns and mysids, while adult fish prey on other fishes, including mugilids, sillaginids, and sciaenids, and occasionally smaller conspecifics. This species is primarily found along the East and South China Sea coasts, as well as in Vietnam and Thailand, and it has also been recorded in Japan (Motomura 2004). In China, *E. rhadinum* juveniles and larvae have been found between June and September in Hangzhou Bay estuary, salt marshes, and tidal flats of the Yangtze River estuary, and sandy beach zones of the Zhoushan Islands (Jin et al. 2007, 2010, Quan et al. 2009a,b, Mao et al. 2013, Chen et al. 2015, Huang et al. 2017). *E. rhadinum* holds considerable commercial and recreational value for gillnet, set net, and rod and reel fisheries in coastal and inshore waters of China due to its exceptionally high auction price in fish markets (Motomura 2004, Su et al. 2020). It has been extensively exploited in China. Currently, a summer fishing moratorium is applicable to nearly all commercial fishing gears in coastal and inshore waters of China (Huang & He 2019). However, specific management measures targeting this species and its critical habitats are lacking. In recent decades, over-exploitation of fishery resources, along with increasing environmental pollution and degradation of critical habitats in nearshore waters, have led to a decline in the fishery resources of the Polynemidae family (Lin et al. 2015). Understanding the utilization patterns of key habitats in the life history of a species can facilitate the formulation of targeted conservation measures.

Life history construction based on otolith microchemistry has suggested that *E. rhadinum* spawn in nearshore waters, with juveniles entering estuarine areas before moving to nearshore habitats to over-

winter (Xuan et al. 2022). *E. rhadinum* is a warm-water species, with year-round distributions in Hainan, Guangdong, southern Fujian, and southern Taiwan (Su et al. 2020). However, its occurrence along the temperate coastlines of Jiangsu and Zhejiang in China is restricted to the summer and autumn months. This suggests that this species migrates to overwintering grounds. Yet, the exact overwintering locations of the populations from Jiangsu and northern Zhejiang remained elusive. Furthermore, it is unclear whether these fish return to their original habitats after overwintering or if they potentially remain in the warmer southern regions. Therefore, the objective of this study was to describe the extent to which fish move among origin and overwintering locations, using the chemistry (trace elements and stable isotopes) of otoliths collected from juveniles and adults. By analyzing the core characteristics of juvenile fish otoliths, we established a baseline to facilitate the categorization of adult samples. This baseline enabled us to trace the shifts in habitat use as the fish progressed through different life stages. We specifically tested the hypothesis that juvenile *E. rhadinum* in the northern region migrated to southern regions for overwintering, where they mixed with individuals from other regions, and then migrated to East China Sea coastal areas in the following year.

2. MATERIALS AND METHODS

2.1. Sample collection

Eleutheronema rhadinum is distributed along coastal areas of China, from Rudong in northern Jiangsu to Hainan Island (most southern part), covering 3 ecoregions: the East China Sea (ECS), South China Sea (SCS), and Beibu Gulf (BG) ecoregions (Fig. 1). Juvenile and adult fish were collected in each ecoregion from commercial gillnet fisheries. In the ECS, juvenile fish were captured in November 2021 in Xiangshan (XS) and August 2022 in Rudong (RD),

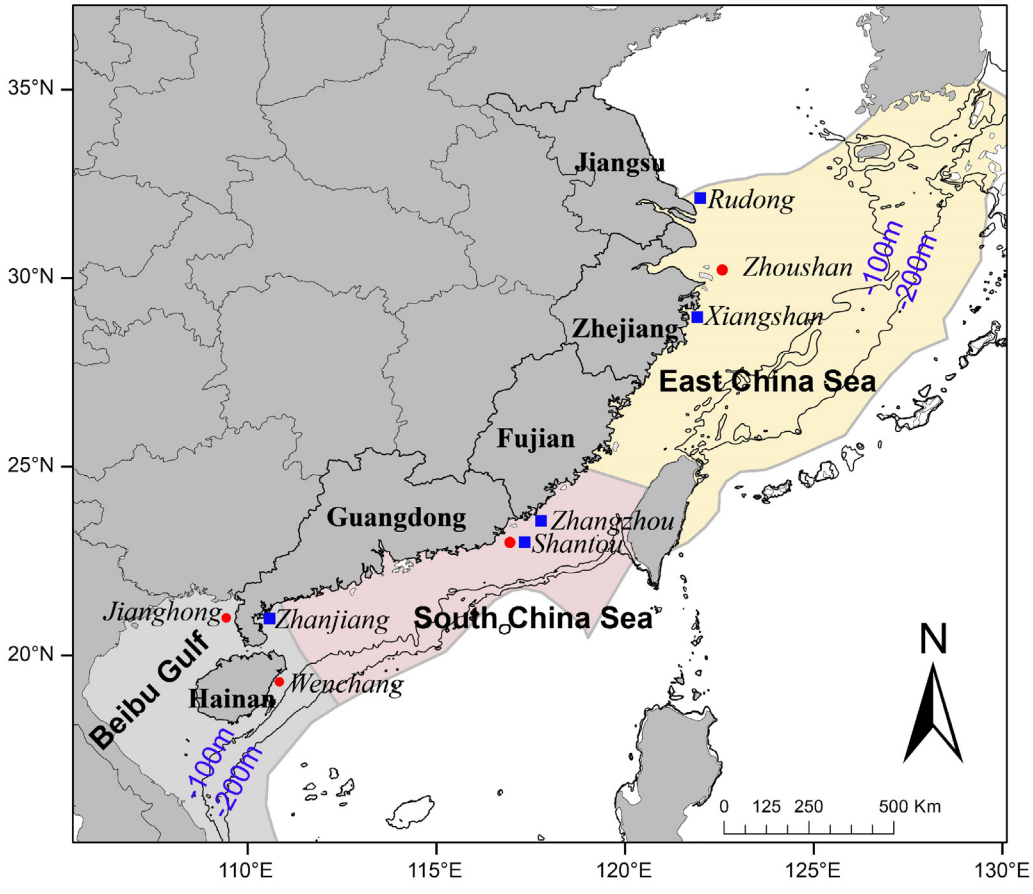

Fig. 1. Ecoregions and sampling locations for *Eleutheronema rhadinum* in the China Sea. The East China Sea ecoregion is in the Warm Temperate Northwest Pacific Province of the Temperate Northern Pacific Realm, whereas the South China Sea and Beibu Gulf ecoregions are in the South China Sea Province of the Central Indo-Pacific Realm. Red circles: adult populations; blue squares: juvenile populations

while adult fish were caught by fishermen in Zhoushan (ZS) in May–June 2022. In the SCS ecoregion, juvenile fish were caught by fishermen in Zhangzhou (ZZ) and Shantou (ST) in November 2021, and adult fish were captured in ST in April 2022. In the BG ecoregion, juvenile fish were caught by fishermen in Zhanjiang (ZJ) in November 2021, and adult fish were captured in Wenchang (WC) and Jianghong (JH) in February 2022 (Table 1). Fish were collected during 2–3 fishing operations. The fishing vessels operated in the waters near the port, typically not venturing out for more than 3 d. The fishing operations were conducted within a radius of no more than 50 nautical miles. Hence, while the collection involved multiple fishing operations, they were concentrated in a relatively localized area within each ecoregion. Monthly averaged sea surface temperatures at the sampling points were obtained from the WHOI Global Ocean Surface Dataset (Fig. 2). The sea surface temperatures of the ecoregions where the sampling sites were located were related to their suitability for *E. rhadinum* overwintering. Sampled fish were immediately frozen at −20°C and transported back to the laboratory. Total length (TL, to the nearest mm) and fork length (FL, to the nearest mm) were also recorded, and sex was determined during dissection. DNA was extracted, and the species was identified as *E. rhadinum* using cytochrome c oxidase subunit I (https://planetarycomputer.microsoft.com/dataset/noaa-cdr-sea-surface-temperature-whoi-netcdf).

Table 1. Sampling locations of juvenile and adult *Eleutheronema rhadinum* collected in China and sample characteristics. N: number; FL: fork length (mean ± SD)

Location	Abbreviation	Sampling date (yr/mo)	N	FL (cm)
Juvenile				
Rudong	RD	2022/08	20	12.5 ± 0.7
Xiangshan	XS	2021/11	25	27.6 ± 1.1
Zhangzhou	ZZ	2021/11	20	27.6 ± 2.9
Shantou	ST	2021/11	14	27 ± 1.6
Zhanjiang	ZJ	2021/11	18	26.8 ± 1.7
Adult				
Zhoushan	ZS	2022/05–06	23	47 ± 3.1
Shantou	ST	2022/04	20	46.7 ± 4.0
Jianghong	JH	2022/02	16	46.6 ± 2.9
Wenchang	WC	2022/02	4	48 ± 1.6

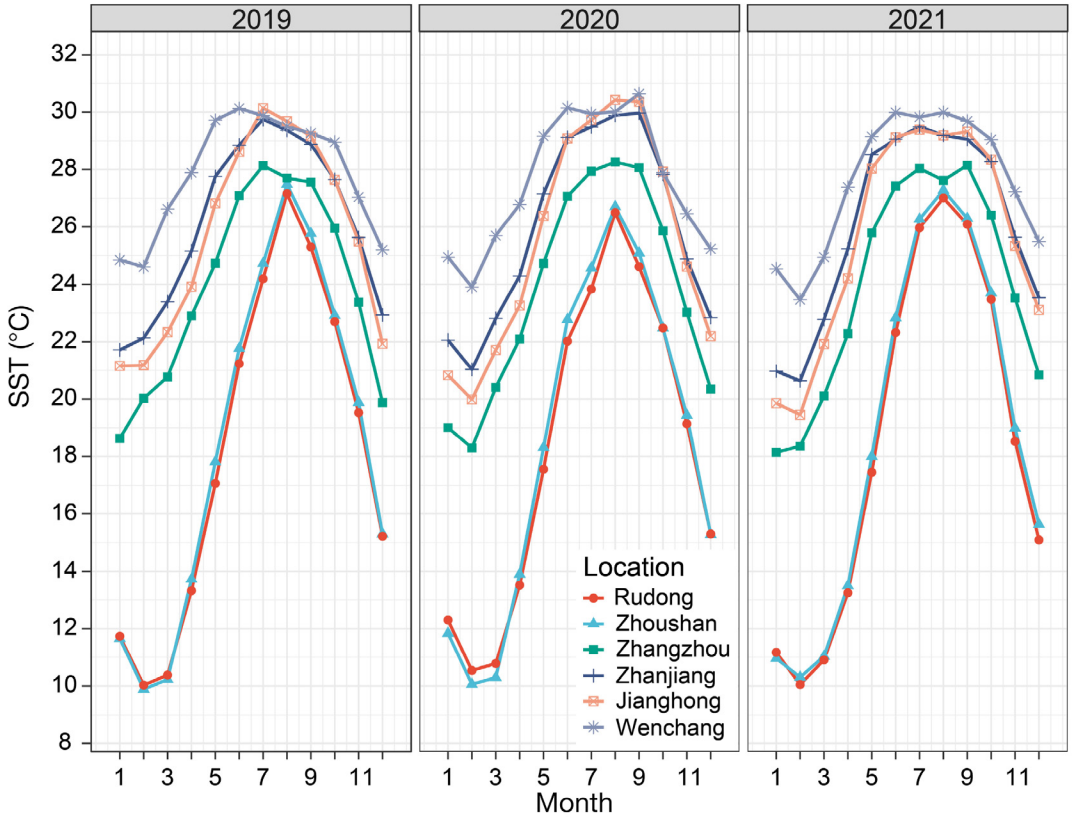

Fig. 2. Monthly average sea surface temperature (SST) for the sampling sites (note no data available for sites Xiangshan and Shantou). Original data were from the WHOI Global Ocean Surface Dataset (https://planetarycomputer.microsoft.com/dataset/noaa-cdr-sea-surface-temperature-whoi-netcdf)

2.2. Otolith microchemistry and stable isotope analysis

The sagittal otoliths were extracted from each individual fish. After washing and drying, the right sagittal otoliths were used for linescan analysis to obtain the life-time elemental profiles of each fish. Following an established protocol (Xuan et al. 2022), the right sagittal otoliths were embedded in epoxy resin (Struers), then cross-sectioned in the transverse plane with a precision slow-speed circular saw (Buehler). The otolith core was preserved in each otolith slice with a thickness of 0.7–0.8 mm, and was then ground until the otolith core appeared. The left sagittal otoliths were used for the core element and stable isotope analysis. The left sagittal otoliths were embedded in epoxy resin with the distal surface side up, then the sagittal plane was ground to expose the core. For both right and left otoliths, otolith surfaces were polished with silica suspension using a LaboPol-35 automated polishing wheel (Struers) prior to analysis, then ultrasonically washed with ultrapure water (Millipore) for 5 min.

Otolith element concentrations were obtained by a laser ablation–inductively coupled plasma–mass spectrometry (LA-ICP-MS), i.e. an NW213 laser ablation unit (New Wave Research) coupled to an Agilent 7500ce inductively coupled plasma mass spectrometry (ICP-MS) (Agilent Technologies). An atmosphere of pure helium (He gas flow 800 ml min^{-1}) in the sealed ablation chamber minimized the re-condensation of ablated materials and elemental fractionations. Two standards, i.e. NIST 612 (National Institute of Standards and Technology, USA) and MACS-3 (United States Geological Survey), were ablated at the beginning and end of each analysis round (every 30–35 min). For the linescan analysis, ablation was conducted with a laser firing rate of 10 Hz, ablation diameter of 50 µm along the transects with the sample stage moving at 10 µm s^{-1}. For the core element analysis, 5 spots along a line were ablated (spot size 50 µm, distance between center of spots 60 µm, dwell time = 5 s, wash-out time = 5 s), and the center of the third spot covered the otolith primordium. Due to the lack of detailed information on the duration of the *E. rhadinum* larval stage, information from the closely related species *E. tetradactylum* was used as a reference (Xuan & Wang 2023). The 5 laser-ablated spots spanned 120 µm on the left and right sides of the primordium, corresponding to the larval stage. Following the methods proposed by Mischel et al. (2017), raw instrument intensity data were converted to elemental concentrations. The otolith elemental concentrations were standardized to calcium and converted to molar concentrations (Morissette & Sirois 2021).

The left sagittal otolith was repolished prior to isotope analysis to remove the laser ablation burn scars, and was then ultrasonically cleaned with ultrapure water for 5 min. After washing and drying, each left sagittal otolith was drilled with a MicroMill microsampling system (New Wave Research) in the central part of the nucleus area. The diameter of the drilling hole was 300 µm (corresponding to the range of the 5 laser ablation spots in the left sagittal otolith), while the depth was set to 100 µm, which was estimated as approximately 15 d based on a previous study (Su et al. 2020). Drilled otolith powder samples were carefully collected (approximately 50 µg per specimen) and placed at the bottom of glass test tubes for stable isotope analysis using a Delta V Advantage stable isotope ratio mass spectrometer equipped with a Gas Bench II Gas generator (Thermo Fisher Scientific), following previously reported methods (Jiang et al. 2022). Isotope ratios are reported using δ-notation with respect to the Vienna Pee Dee Belemnite (VPDB) standard, using international standards NBS-18 and IAEA-603 (International Atomic Energy Agency). Before measuring the samples, a primary test was performed by analyzing a series of 6 standard samples (3 pairs) to validate the machine conditions. During the main run, a pair of standards was placed between every 10 samples. The analytical precision based on the measurements of standards were better than 0.05‰ for both $\delta^{13}C$ and $\delta^{18}O$ values.

2.3. Age determination

After the microchemical analysis, the surface of the right sagittal otolith was etched with 5% ethylenediaminetetraacetate (EDTA) (pH 7.5, buffered with KOH) to reveal the annuli of the otolith samples. During etching, reflected-light microscopy was used to monitor the quality of the etching to avoid destruction of the samples by etching. A digital Olympus BX51 microscope camera and coupled imaging system was used to take the otolith photographs, and to measure the length from the otolith core to the annulus marks along the laser ablation line. A previous study validated the otolith annuli of *E. rhadinum*, and individuals were successfully aged through otolith microstructure (Su et al. 2020). The ages of the individual samples were determined in this study from the otolith annuli according to Su et al. (2020).

2.4. Life history reconstruction

Sr:Ba ratio profiles from otolith linescan analysis were used to reconstruct the life history of *E. rhadinum*. Some studies indicate that the Ba:Ca ratio is a good indicator of transitions between estuarine and marine environments, and it was used in previous studies of *E. rhadinum* (Menezes et al. 2021, Russell et al. 2022, Xuan et al. 2022). However, the literature also suggests that Sr:Ba ratios are particularly sensitive to transitional environments such as estuaries (McCulloch et al. 2005, Baker et al. 2019). Given the heightened sensitivity of Sr:Ba ratios in indicating transitions between estuarine and marine environments, we utilized Sr:Ba to investigate the transitions of *E. rhadinum* between estuarine and coastal habitats. The distance from the otolith core can be indicative of age; however, due to individual variations and differences in growth stages, the relationship between distance and age differed across individuals and at different stages of life. Therefore, we opted to use 'distance from the core' as the coordinate axis for the elemental profile. Change-point analysis was performed to identify the portion of the otolith when there was a change in Sr:Ba ratio representing a change in otolith chemistry, following the pruned exact linear time (PELT) algorithm with the 'changepoint' package in R. The PELT algorithm automatically divides the profile at multiple points where statistically significant changes occur based on variations in mean and variance. This algorithm is somewhat more computationally efficient than other algorithms (Killick & Eckley 2014). The average ratio was calculated within each segment. It is important to note that a stable Sr:Ba value could mean (1) the fish is not moving and the isotopes in the water are stable, (2) the fish is moving but remains within a parcel of water that has stable levels of measured isotopes, or (3) some combination of 1 and 2. Changing Sr:Ba values could mean (1) the fish is moving between areas with different isotope concentrations, (2) the fish is stationary and water flowing past it contains differing isotope concentrations, or (3) some combination of 1 and 2.

2.5. Variation in natal area geochemistry

The average values of the ratios of elements:Ca and the ratios of carbon and oxygen isotopes from the 5 laser-ablated points were considered to represent the natal area geochemistry of an individual fish. The potential disparities among the 5 juvenile fish groups were assessed. Prior to the comparisons, the normality of variances was verified using the Shapiro-Wilk test. Given that many variables exhibited non-normal distributions, Levene tests, which are less sensitive to deviations from normality, were employed to test the homogeneity of variances. Despite attempts to normalize the data through Box-Cox transformation, only the Mn:Ca ratio and $\delta^{13}C$ values fit a normal distribution and homogeneity of variance. Henze-Zirkler's test was applied to test the multivariate normality of the juvenile otolith core data set. Because the data set of juvenile fish did not meet multivariate normality, a permutational multivariate analysis of variance (PERMANOVA) was performed to check whether there were significant differences among the juvenile groups. To meticulously control Type I errors arising from multiple comparisons during pairwise PERMANOVA, between every group pairing, the 'p.adjust' function in R was employed with the Bonferroni method to adjust the p-values. An adjusted p-value <0.05 was considered statistically significant.

To identify the potential distinct natal ecoregions, we employed unsupervised approaches, which grouped samples exhibiting similar attributes without previous classification, to cluster the otolith core multielement and stable isotope data from early life history stages of *E. rhadinum*. Because the juvenile fish from ST were collected after adults, they were not used for the following analysis. The otolith core multielement and isotopic data were Z-score normalized, then hierarchical clustering was carried out by employing a similarity matrix based on Manhattan distance. The optimal number of clusters was determined by the Hubert index, and the D index was calculated using the 'NbClust' function in the 'NbClust' package. The clustering results, along with the normalized multielement and isotopic data, were visualized using the 'heatmap' function within the 'heatmap' package. The R package 'kohonen' was used to generate self-organizing maps (SOMs), which were dimensionality-reducing and topology-preserving mappings of input variables, to arrange samples with similar characteristics into identical or adjacent nodes. However, the SOMs did not provide information on subsets of node clusters. To assign the SOM output nodes to different clusters and confirm the optimal number of divided clusters of the entire sample sets, hierarchical clustering analysis was applied for the weights of those nodes. The core chemical composition and isotope ratios were also investigated by nonmetric multidimensional scaling (nMDS) utilizing the 'vegan' package in R. The construction of the dissimilarity matrix was based on Manhattan distances, and assessment of the goodness-of-fit was carried out using the stress value.

2.6. Natal assignment

We employed the 'mlr' package in R to explore various classification models, including linear discriminant analysis (LDA), quadratic discriminant analysis, random forest, and classification and regression trees based on otolith core data of juvenile fish from known ecoregions, to ascertain which classification model is more appropriate for our data set (Smoliński et al. 2020). We evaluated all possible combinations of different models and variables, ranging from a single variable to the inclusion of all variables, to identify the model that yields the highest accuracy and kappa value. We utilized 10-fold cross-validation to assess the accuracy of models in classifying juvenile fish to their known capture sites, and ultimately selected the LDA model with all variables, as it exhibited the highest classification accuracy and kappa value. LDA is a method of classification that creates linear discriminant functions to distinguish products from different groups. It operates by maximizing the variance between groups while simultaneously minimizing the variance within each group (Sharma & Paliwal 2015, Han et al. 2021). The LDA model was developed from juvenile fish otolith core signatures to assign the adult fish to natal areas. Thus, the signatures of juvenile fish otolith cores were treated as the training data to construct the LDA model. The juvenile fish otolith core data set was randomly segmented into 10 subsets, with 9 used to train the model, and the remaining set used to assess the predictive capabilities of the model; this procedure was iteratively performed 10 times. The entire process was repeated 20 times to ascertain the mean classification accuracy of the model. Subsequently, employing the previously established LDA model, the otolith core signals from adult fish were used as test data to calculate the probability of adult fish belonging to a group (without prior geographical location information). The LDA calculated the probabilities of individual fish belonging to source populations, thereby predicting individual origins rather than estimating the overall population mixing ratio.

To estimate the composition of the mixed groups (adult fish), otolith core element and isotopic baselines of juvenile fish from 3 different ecoregions were utilized as references to assign the otolith core of adults (representing the hatching period) to the natal origin. The natal origin of adult fish was identified using the HISEA program to execute maximum likelihood estimation (MLE) analyses (HISEA available at https://www.stat.auckland.ac.nz/~millar/mixedstock/code.html; Millar 1987, 1990). The HISEA bootstrap procedure was applied to assign natal origin, and the composition estimate means and standard deviations of the proportion of each mixed stock originating from each characterized baseline group were obtained using 1000 simulations.

3. RESULTS

3.1. Otolith elemental ratios

In this study, a total of 160 *Eleutheronema rhadinum* were collected, comprising 97 juveniles and 63 adults with FLs ranging from 11.3 to 29.3 cm and 40.9 to 52.7 cm, respectively (Table 1). All juveniles had not yet formed their first annulus, while the adults had already formed one. The Sr:Ba ratios in *E. rhadinum* ranged from 13.71 to 2343.7. Almost all otoliths had a Sr:Ba ratio of less than 500 in and near the core, rising sharply after a certain distance, and the distance between the otolith core and the starting point of the sudden increase in Sr:Ba ratio varied among different ecoregions and even within the same ecoregion. Among the juvenile fish, individuals from RD exhibited the smallest ages and correspondingly lower Sr:Ba ratios. In ZJ, 2 individuals displayed a significant increase in Sr:Ba values (exceeding 500) within a distance of 150 µm from the otolith core, while the majority of *E. rhadinum* experienced a substantial rise in Sr:Ba ratios at distances between 300 and 650 µm from the core. In ZZ, XS, and ST, the majority of individuals displayed a significant increase in Sr:Ba values (exceeding 500) at a distance of about 300 µm from the otolith core. Among the adult fish, individuals from WC exhibited a relatively long distance from the core with a low Sr:Ba ratio. In ZS, ST, and JH, the majority of individuals displayed a significant increase in Sr:Ba values (exceeding 500) within a distance between 300 and 650 µm from the core (Fig. 3).

3.2. Otolith elemental and stable isotope ratio composition

A total of 97 juvenile otoliths were analyzed from 5 distinct locations to characterize the geochemical features of potential natal sites. In juvenile fish otoliths, Li:Ca ratios ranged from 0.0011 to 0.0075 mmol mol^{-1}, Na:Ca ratios from 10.521 to 13.80 mmol mol^{-1}, Mn:Ca ratios from 0.0011 to 0.0113 mmol mol^{-1}, Sr:Ca ratios from 1.15 to 2.51 mmol mol^{-1}, Ba:Ca ratios from

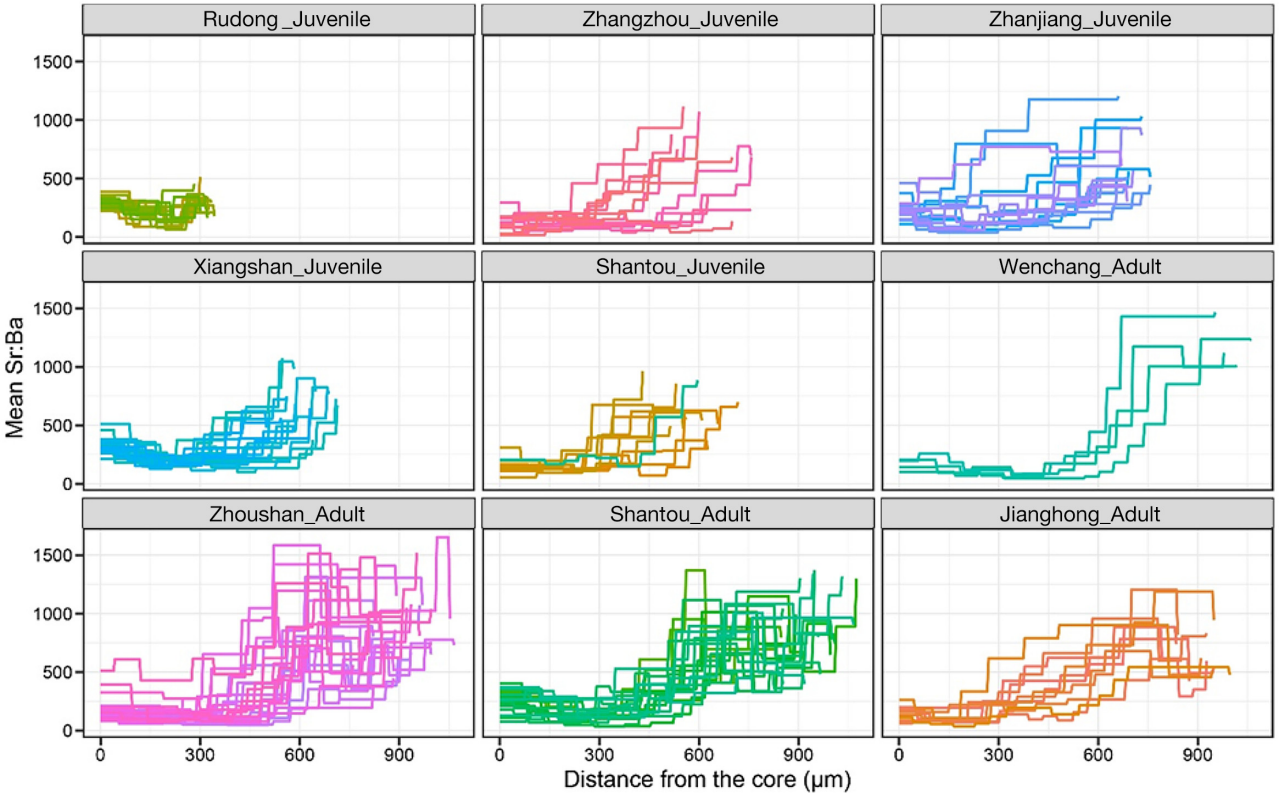

Fig. 3. Mean Sr:Ba profiles along otolith growth axes for juvenile and adult *Eleutheronema rhadinum* collected at different sampling sites. The Sr:Ba ratio of each individual was divided into different segments based on the changepoint analysis. The mean Sr:Ba values of each segment are displayed to indicate possible changes in the corresponding habitat conditions. Different colors indicate different individuals

0.0051 to 0.0588 mmol mol^{-1}, Sr:Ba ratios from 31.97 to 413.97 mol mol^{-1}, $\delta^{13}C$ from −12.00 to −5.11‰, and $\delta^{18}O$ from −9.75 to −3.66‰ (Fig. 4). No significant difference was observed in all elements and isotopes between ST and ZZ, while significant differences in Li:Ca and Sr:Ba ratios were found between RD and XS, with no significant difference in other elements and isotopes. ZJ exhibited significantly lower Na:Ca ratios, Mn:Ca ratios, and $\delta^{13}C$ and $\delta^{18}O$ values compared to the other 4 juvenile groups. In contrast, among the adult groups, there were almost no significant differences in elements and isotopes between groups, but intra-group variation was more pronounced (Fig. 4).

The pairwise comparison results from non-parametric PERMANOVA demonstrated that there were no significant differences between juveniles from RD and XS, or between juveniles from ZZ and ST. All other pairwise comparisons between groups displayed significant differences (Table 2).

Based on the normalized elemental and stable isotope ratios of juvenile fish otoliths, hierarchical clustering revealed 3 primary clusters: XS formed a distinct cluster, ZZ and ST together made up one cluster, and ZJ formed a separate cluster that included some individuals from ZZ and ST. The XS cluster was not mixed with other locations (Fig. 5a). The optimal grouping of clusters for the otolith core data of juvenile fish after dimensionality reduction using SOM resulted in 2 clusters: XS from the ECS ecoregion was one cluster, and ZZ, ST from the SCS ecoregion, and ZJ from the BG ecoregion formed another cluster (Fig. 5b). The nMDS results showed that individuals were primarily divided into 3 clusters. When plotting the boundaries according to the capture locations of individuals, ZZ and ST overlapped, and XS and ZJ each formed a separate cluster, creating 3 distinct primary regions. Therefore, juvenile fish from these 4 locations could be divided into 3 main clusters, and geographically proximate groups were grouped within the same cluster, ultimately corresponding to the 3 major ecoregions (Fig. 5c). We designated the juvenile fish from XS as the ECS unit, those from ZZ and ST as the SCS unit, and those from ZJ as the BG unit.

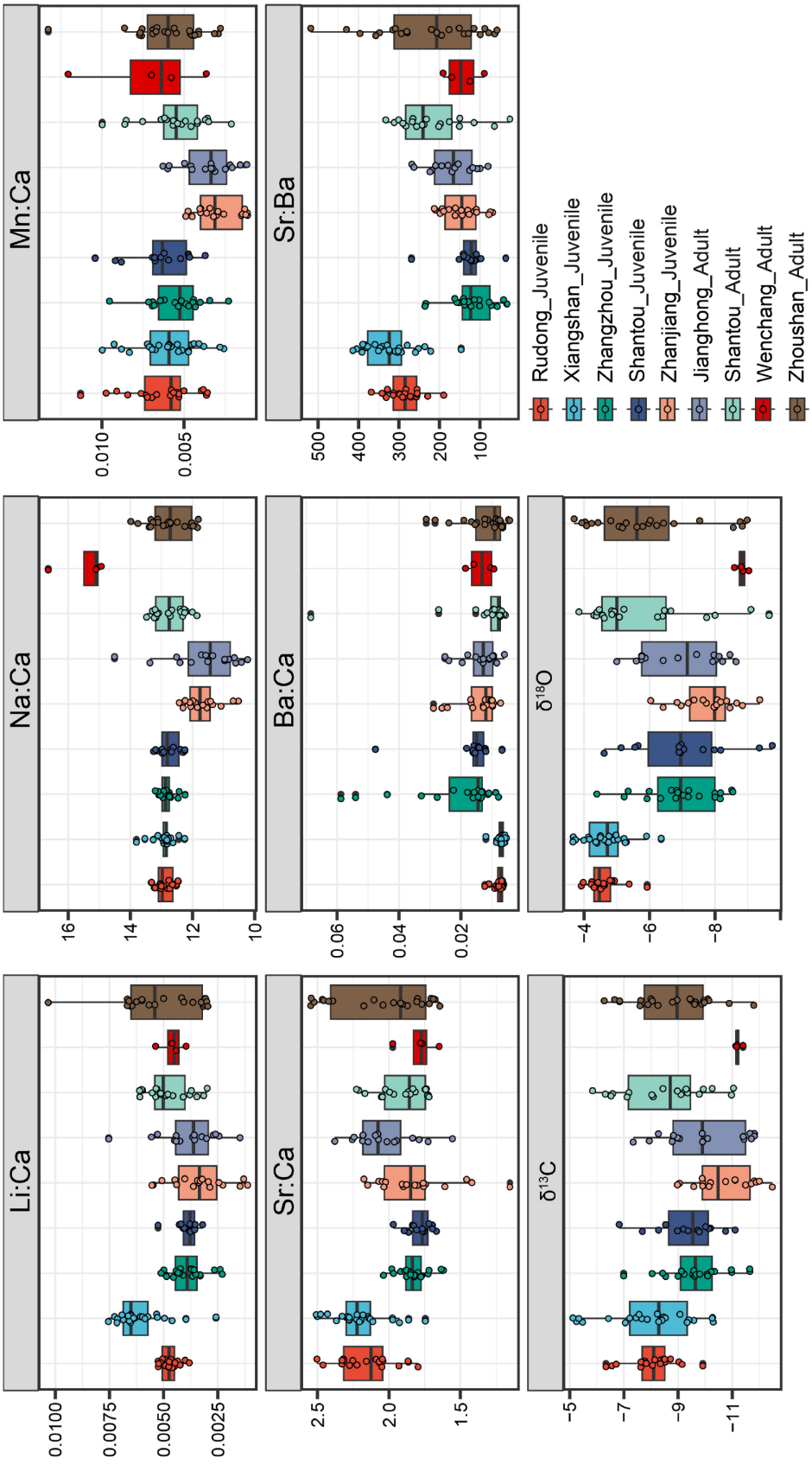

Fig. 4. Elemental concentrations and stable isotopes ratios in otolith cores of *Eleutheronema rhadinum* from different sampling groups. Horizontal line in box: mean value; bottom and top of box: 25th and 75th percentiles; whiskers: 5th and 95th percentiles

Table 2. p-value matrix of pairwise PERMANOVAs between every juvenile fish group pairing. *: significant difference between groups ($p < 0.05$); ns: no significant difference ($p > 0.05$)

	Rudong	Jiangshan	Zhangzhou	Shantou	Zhanjiang
Rudong					
Xiangshan	0.305^{ns}				
Zhangzhou	0.001*	0.001*			
Shantou	0.001*	0.001*	0.727^{ns}		
Zhanjiang	0.001*	0.001*	0.001*	0.001*	

3.3. Classification accuracy of the core portion of juvenile and adult otoliths

Juvenile fish from 4 sampling sites not including RD were classified into 3 ecoregions, and the LDA model with all variables exhibited the highest classification accuracy and kappa value (Fig. 6). The classifier constructed using LDA exhibited a classification accuracy exceeding 98.3% among the 3 ecoregions. The 2-

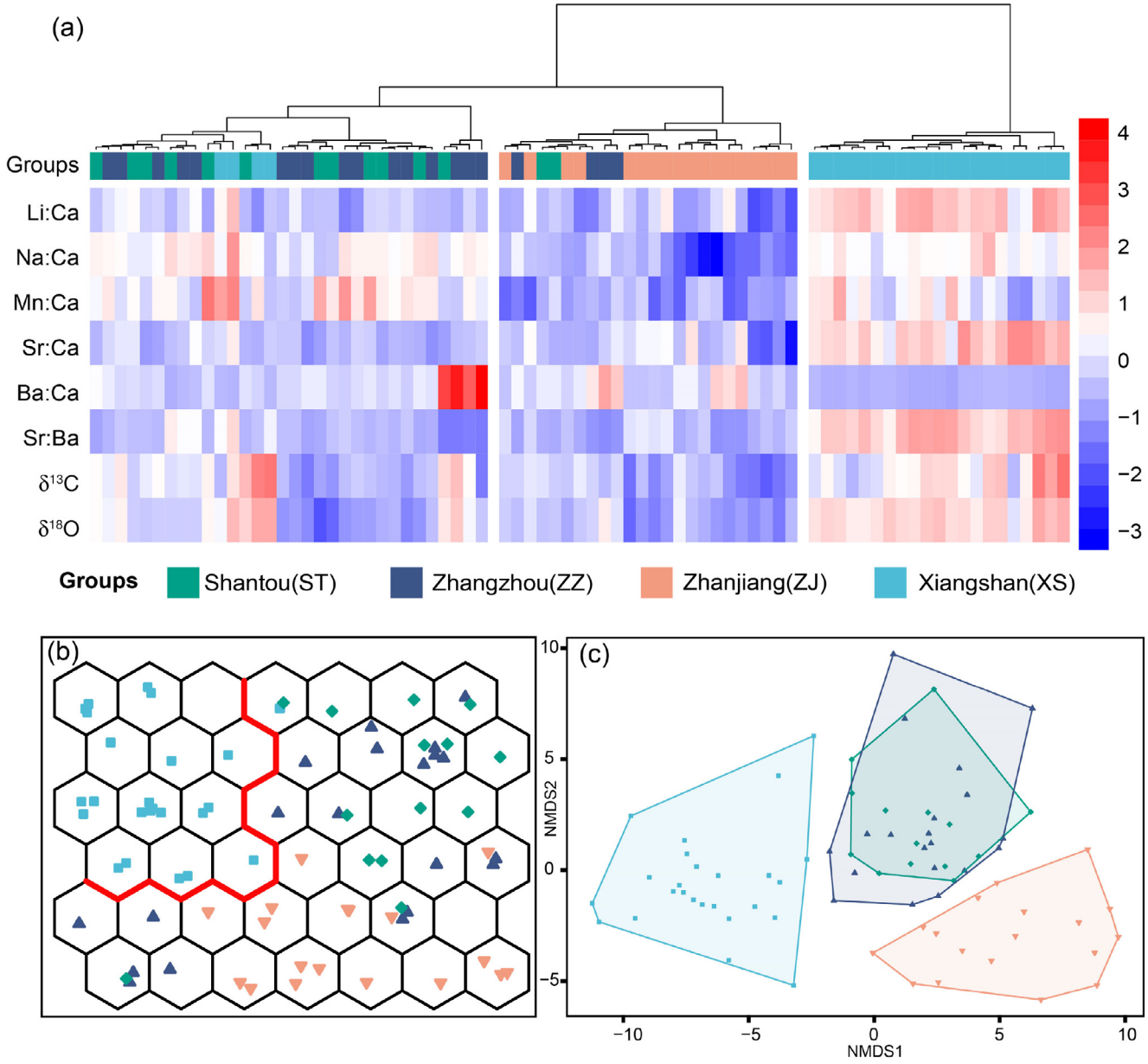

Fig. 5. Output of unsupervised approaches for the juvenile fish from 4 different sampling sites: (a) hierarchical clustering analysis; (b) self-organizing maps (the thick red line differentiates between 2 clusters); (c) nonmetric multidimensional scaling (NMDS). Groups refer to locations where fish were sampled

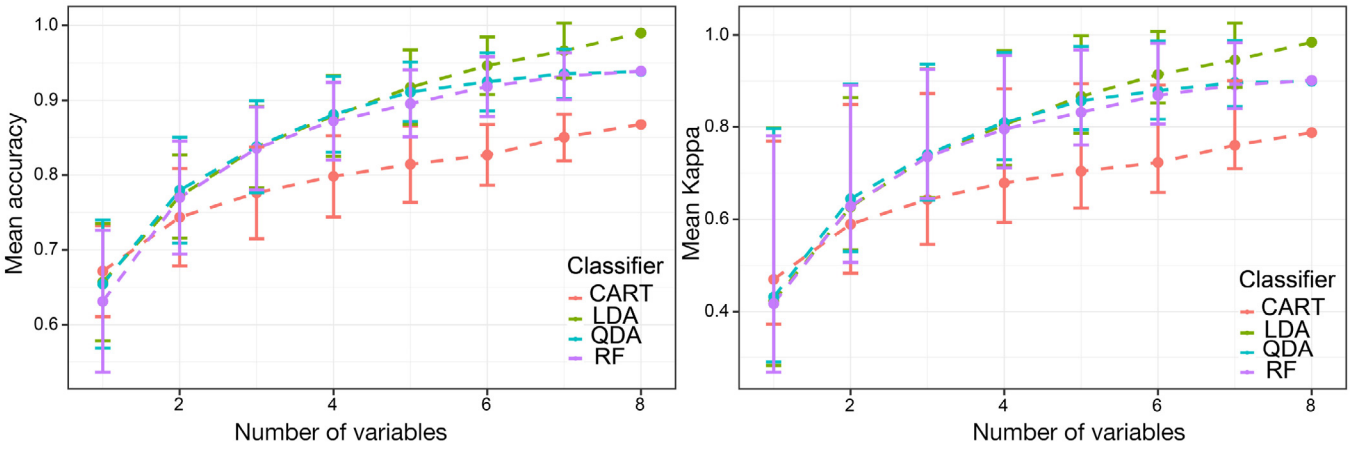

Fig. 6. (a) Classification accuracy and (b) kappa values of different statistical models based on different numbers of variables. Lines represent median accuracy and kappa values, respectively, and error bars represent SD. CART: classification and regression trees; LDA: linear discriminant analysis; QDA: quadratic discriminant analysis; RF: random forest

dimensional distribution plot of the discriminant functions displayed clear boundaries between the ecoregions (Fig. 7). Based on otolith core signals, the LDA model based on juvenile fish was used to classify the adult fish to their ecoregion origin. The posterior probabilities for each adult fish with respect to the 3 ecoregions were calculated, and individual fish were classified into an ecoregion when its posterior probability of belonging to that region exceeded 95%. If the posterior probabilities did not reach 95%, the individual fish was deemed to potentially not belong to any of the 3 geographical regions. Among the adult fish, 11 individuals did not reach the threshold and were considered as being of indeterminate origin. The remaining adult fish were assigned to distinct ecoregions (Fig. 8).

The LDA revealed a complex origin structure among adult fish groups. All 4 adults from WC originated from SCS. In JH, 3 out of 16 adults were from the SCS, 1 from the ECS, and the remainder from the BG. For the 24 adults from ST, origins of 3 were unidentifiable, 15 were ECS, 1 BG, and 5 SCS. For the 19 adults from ZS, 9 had indeterminate origins, 3 were SCS, and 7 were ECS (Fig. 9). MLE indicated that the JH adult fish primary originated from BG, accounting for 76%. ST mainly originated from ECS (59%), with SCS contributing to 35%. All individuals from WC were from SCS. ZS individuals were primarily from ECS, with similar contributions from SCS and BG (Table 3).

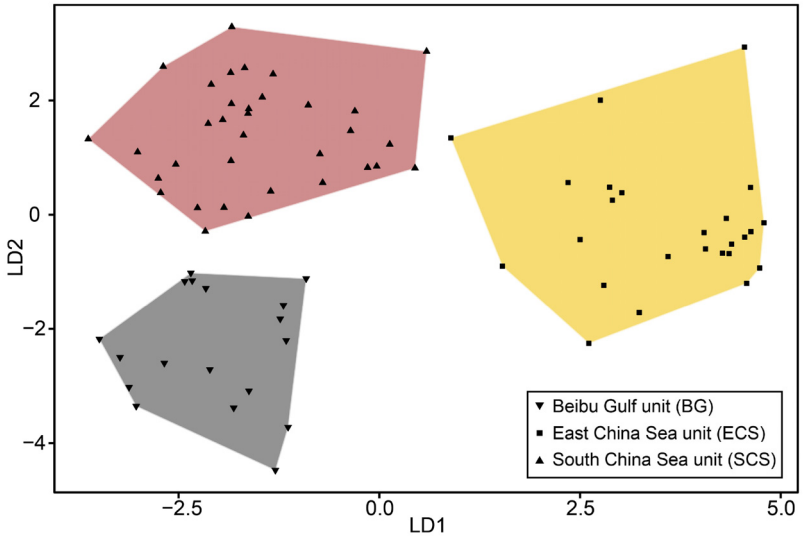

Fig. 7. Plots of the first and second canonical variables from the discriminant function analysis for juvenile *Eleutheronema rhadinum*. Juveniles collected from the same ecoregion belong to the same group and have the same symbol shape and background color

4. DISCUSSION

This study employed otolith elemental compositions and stable isotopes to assess the life history, population connectivity, and migratory patterns of *Eleutheronema rhadinum* across different ecoregions along the coast of China. Juvenile fish from 3 distinct ecoregions showed that otolith core elemental and isotopic characteristics differed significantly, with

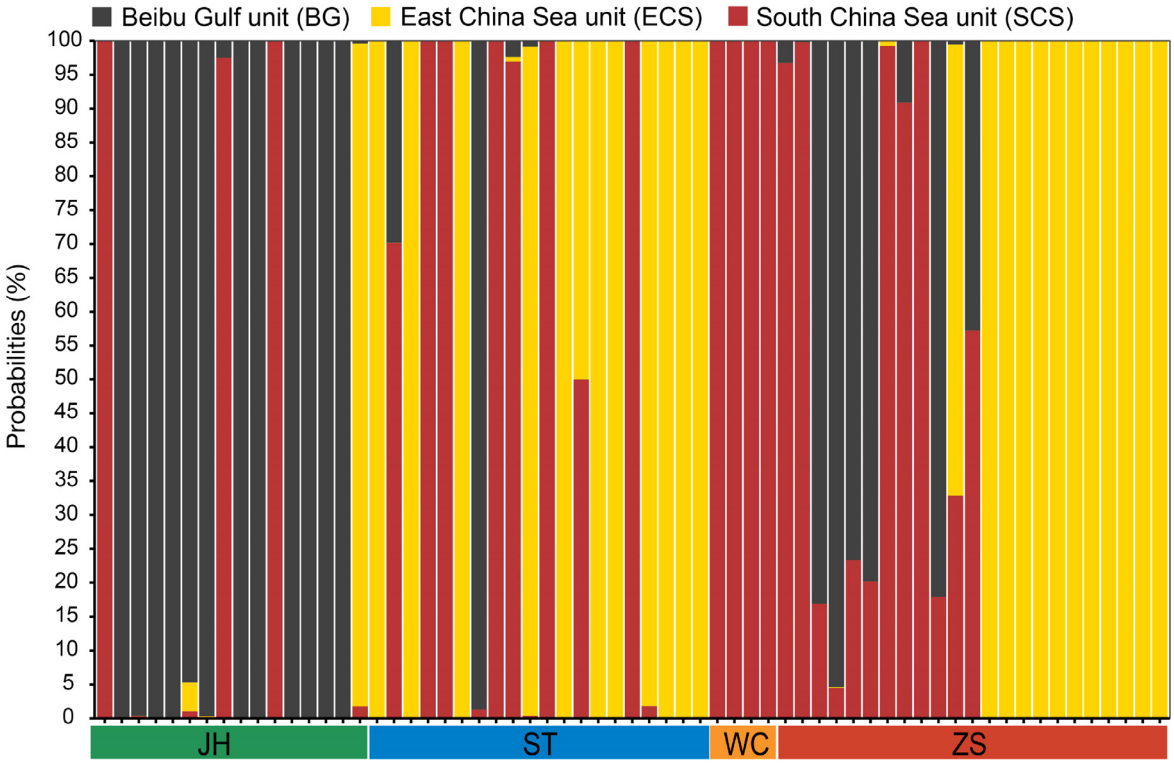

Fig. 8. Probability of adult *Eleutheronema rhadinum* individuals assigned to different ecoregions according to otolith core signals. The *y*-axis shows the individual-specific cumulative posterior probability of assignment to each of the 3 ecoregions. Individuals are ordered along the *x*-axis, the color below the *x*-axis indicates where the adult fish were caught. JH: Jianghong; ST: Shantou; WC: Wenchang; ZS: Zhoushan

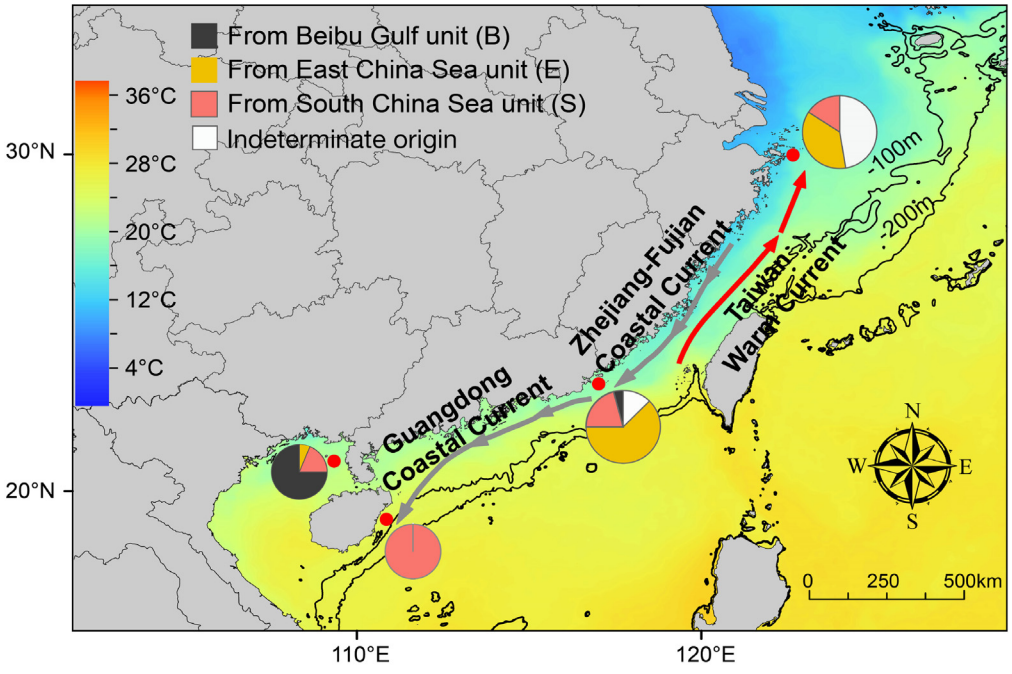

Fig. 9. Contingent composition of the 4 adult *Eleutheronema rhadinum* groups. Pie charts represent the contribution of the 3 ecoregions. Gray and red arrows represent currents. The gradient coloring of the ocean area represents the average temperature in January from 2019 to 2021

Table 3. Maximum likelihood estimates of the relative contributions (%; mean ± SD) of the 3 ecoregions for adult *Eleutheronema rhadinum*. JH: Jianghong; ST: Shantou; WC: Wenchang; ZS: Zhoushan; ECS: East China Sea; SCS: South China Sea; BG: Beibu Gulf

Natal origin	Adult fish sampling sites			
	JH	ST	WC	ZS
ECS	5.93 ± 6.06	59.07 ± 11.29	0	50.96 ± 10.78
SCS	17.63 ± 9.97	34.86 ± 11.40	100 ± 0	28.51 ± 11.47
BG	76.44 ± 11.05	6.08 ± 5.91	0	20.53 ± 10.23

over 98% of juvenile individuals being correctly assigned to their ecoregions. Based on the LDA model constructed by the otolith core elements and stable isotope ratios of juvenile fish, adult fish were assigned to their respective potential natal ecoregions. The results suggested that some fish from the SCS and BG ecoregions derived from the ECS. Juvenile fish disappeared from the ECS during winter: by late spring of the following year, *E. rhadinum* from the ECS were found in the SCS and BG, areas which were suitable for their overwintering, indicating that the SCS and BG ecoregions may serve as wintering grounds for *E. rhadinum* from the ECS. Additionally, the northward migrating populations in summer included individuals from the SCS, indicating connectivity among the distinct ecoregions.

4.1. Differences in otolith microchemistry across ecoregions

We examined the otolith core elemental and stable isotope characteristics of *E. rhadinum* across 3 ecoregions. The elemental and isotopic signals of the otolith core represented the larval stage, potentially corresponding to the spawning and nursery grounds rather than the sampling locations. The juvenile fish we collected had already moved to nearshore habitats, and potentially originated from various spawning and nursery grounds. The elemental and isotopic signals of the otolith core represented these grounds rather than the actual sampling locations. Moreover, the timing of entry into the marine environment varied both between different locations and within the same location, with potential driving factors including temperature, food abundance, and the distance from the spawning ground to the estuary (Baker et al. 2019, Menezes et al. 2021). This warrants further investigation in future studies.

The results of the present study showed that the elemental and stable isotope features of the juvenile fish otolith cores were distinctly different among ecoregions. The differences were likely attributable to the environmental variations among these ecoregions (e.g. salinity, upwelling, river discharge, ocean currents, precipitation, and anthropogenic inputs). We observed that the core characteristics of juvenile fish from the same ecoregion were more similar to each other than to those from different ecoregions. This led us to speculate that these fish had not yet undergone extensive migration and mixing, and their spawning and nursery grounds were within the same ecoregion of our sampling locations.

The most noticeable differences between the 3 ecoregions were documented between the ECS region and the other 2 ecoregions. Juvenile fish from the ECS ecoregion exhibited higher Li:Ca and Sr:Ca ratios, and lower Ba:Ca ratios, as well as higher $\delta^{13}C$ and $\delta^{18}O$ compared to the other 2 regions. Li was unlikely to substitute for Ca^{2+} in the aragonite lattice of the otolith (Thomas et al. 2017). However, due to the smaller ionic radius of both Li and Ca, they can randomly enter the gaps in the lattice and bind to otolith crystals (Thomas et al. 2017). Consequently, otolith Li was generally related to the concentration in the surrounding environment, e.g. a positive correlation between otolith Li:Ca ratio and chlorophyll *a* level in the environment (Grammer et al. 2017).

The RD and XS sites were close to the estuary of the Yangtze River, with higher chlorophyll concentrations than the other sites in the SCS and BG ecoregions (Ye et al. 2021). This may explain the higher Li:Ca ratios observed in the ECS ecoregion. Furthermore, a negative correlation between otolith Li:Ca ratio and water temperature was found in European plaice *Pleuronectes platessa* (Sturrock et al. 2015). Juvenile fish collected from XS, ST, ZZ, and ZJ had similar collection times and FLs, suggesting that these juveniles hatched around the same time. During the hatching of larvae, the average temperature of the ECS ecoregion was lower than in the SCS and BG ecoregions, which might contribute to the higher Li:Ca ratios observed in the ECS ecoregion.

Unexpectedly, the RD and XS sites in the ECS ecoregion exhibited higher Sr:Ca and lower Ba:Ca ratios. The Yangtze River has a massive freshwater discharge, causing a widespread influence of freshwater in the river estuary (Patra et al. 2012). In contrast, southern rivers have smaller discharges, resulting in higher salinity in their estuaries (Zhang et al. 2012). If *E. rhadinum* selected similar distances from estuaries for spawning across different regions, RD and XS should

have lower Sr:Ca and higher Ba:Ca ratios. This suggests that *E. rhadinum* spawning in the Yangtze River estuary may choose locations farther away from the estuary. A possible hypothesis to explain this phenomenon is related to the high productivity of the Yangtze River estuary. In such a productive environment, fish can choose to spawn and hatch at locations farther from the estuary, reducing the pressure on eggs and larvae in the estuary as a hotspot of biodiversity. After growing for a certain period, they then enter the estuary nursery grounds, resulting in higher survival rates. However, this hypothesis needs to be further tested with regard to the pelagic larval duration.

The RD and XS sites exhibited higher $\delta^{13}C$ and $\delta^{18}O$ values. Carbon isotope ratios ($\delta^{13}C$) in fish otoliths reflect the dissolved inorganic carbon and diet in the surrounding water (Muto et al. 2022, Sakamoto et al. 2022). Otolith $\delta^{18}O$ is influenced by temperature and the $\delta^{18}O$ of environmental water, making the distribution of seawater $\delta^{18}O$ crucial for estimating temperature using otolith $\delta^{18}O$ (Hsieh et al. 2019, Sakamoto et al. 2022). The scope of this study spans thousands of kilometers from north to south, with differences in latitude leading to variations in temperature and substantial differences in productivity. Therefore, the interplay of multiple factors, such as dissolved inorganic carbon and diet, temperature, and water $\delta^{18}O$, may have led to the large-scale differences in the stable isotope signatures. Further studies with controlled variables are needed to explain the causes of these differences. However, the purpose of using otolith $\delta^{13}C$ and $\delta^{18}O$ as natural biomarkers in this study has been successfully achieved.

4.2. Overwintering migration and natal assignment of adults

After successfully establishing an LDA model for the 3 ecoregions using juvenile fish otolith core signals, we assigned the adult fish to their origins based on their otolith core signals. The results showed that a large proportion of adult fish in the SCS ecoregion during the winter come from the ECS ecoregion, and very few come from the BG ecoregion (only 1 individual, accounting for 4.1%). In the BG ecoregion, all adult fish in WC came from the SCS ecoregion. Only 1 individual in JH came from the ECS ecoregion, few from the SCS ecoregion, while the majority came from the BG region. This indicated that *E. rhadinum* distributed in the south during winter were part of a mixed population. The juvenile fish migrated from the ECS ecoregion to the SCS ecoregion for overwintering; few individuals may travel to even more distant areas.

E. rhadinum is a nearshore benthic fish species, typically inhabiting shallow mud and sandy substrates on the continental shelf, and has never been documented in the vicinity of oceanic islands (Motomura 2004). Therefore, their migration routes were more likely to be from the coastal areas of the ECS along the continental shelf, moving south to the SCS and the BG continental shelf regions for overwintering, rather than heading eastward into the deep sea for overwintering. During the overwintering process, the ECS population may migrate south along the Zhejiang–Fujian coastal current, mixing with the local SCS population at the overwintering grounds (Zheng et al. 2006). The winter marine temperatures in ZZ, ZJ, and JH are not significantly different, and this temperature range was sufficient for *E. rhadinum* to overwinter, while most *E. rhadinum* from the ECS stayed and did not move farther south. However, all 4 adult individuals from Hainan came from the SCS region. Their movement was probably not associated with overwintering, since their natal area may have already satisfied the overwintering conditions. Instead, they were more likely influenced by the Guangdong coastal currents after entering the nearshore environment (Zheng et al. 2006). Moreover, the time at which we collected adult fish in the BG was earlier compared to other locations, yet the size of the fish was similar. This suggested a potential difference in hatching times, with adults in the BG possibly being born earlier than the juveniles used to establish our baseline, posing challenges to interpreting the origins of adult fish in the BG. Fish hatched at different times within the same region may exhibit variations in otolith core elements. Nevertheless, some studies showed that such temporal variations had a limited impact on discrimination between regions (Reis-Santos et al. 2012, Matta et al. 2019). The ZS adult fish samples were collected during the breeding season and included individuals originating from both the SCS ecoregion and the ECS ecoregion. This indicated that some individuals from the ECS ecoregion returned to their natal spawning grounds, although this study was based on a small number of samples and a single sampling event.

Adult fish that originated from the SCS ecoregion appeared in the ECS ecoregion during the breeding season (some reaching reproductive maturity), suggesting that this species does not exhibit strong spawning site fidelity, and the selection of spawning locations is flexible. This indicates that *E. rhadinum* serves as a biological link between the ecoregions of

the SCS and the ECS. While there were some interactions between *E. rhadinum* populations in the BG and those in the ecoregions of the SCS and ECS, the level of exchange was lower than that between the ECS and the SCS. A previous study also showed a certain degree of differentiation between the Pearl River population and the Yangtze River estuary population (Sun et al. 2013).

4.3. Implications for species management

E. rhadinum is primarily distributed along the southern coast of China, with most fishing operations in the region targeting this fishery, although there were a few recorded instances of the species in Japan and Vietnam. Previous studies revealed that *E. rhadinum* relies on estuarine habitats during early life stages (Xuan et al. 2022). In China, many *E. rhadinum* larvae and juveniles were observed in the surf zones, tidal channels, and other habitats around the Yangtze River estuary and Hangzhou Bay during the summer, highlighting these areas as crucial breeding and nursery grounds (Jin et al. 2007, Quan et al. 2009 a,b, Jin et al. 2010, Mao et al. 2013, Chen et al. 2015, Huang et al. 2017). The present study revealed the connectivity between the ecoregions of the ECS and the SCS, as well as the BG. This result implies that the ECS contributes to *E. rhadinum* fishery resources in southern China, which is also a densely populated and important economic activity area in coastal China. Factors such as land occupation for agriculture, aquaculture, and industrial uses, and increasing pollution from agricultural and industrial activities are threatening these crucial aquatic environments (Cao et al. 2020, Wang et al. 2020, Fan et al. 2023). Thus, maintaining and enhancing the remaining intertidal habitats are essential tasks for the conservation of species such as *E. rhadinum* that rely on them as nursery grounds. National policies aiming to control the loss of tidal flats, and intertidal zone action plans are urgently needed to address these cumulative pressures.

This study also revealed the migratory routes between different ecoregions for *E. rhadinum* born in distinct areas, providing information on temporal and spatial migration characteristics, demonstrating the interconnectivity between different ecoregions, which is essential for sustaining fisheries of the species. Maintaining habitat connectivity is critical, and during their concentrated migration, protecting fish when and where they are vulnerable to overharvesting is also crucial (Pease et al. 2023). *E. rhadinum* is a protandrous hermaphrodite, and larger individuals include a higher proportion of females (using the close relative species *E. tetradactylum* as a reference; Shihab et al. 2017). Thus, preventing the overfishing of large individuals during migration might be necessary to avoid detrimental population effects caused by the removal of too many females and large males in this protandrous species (Andrade et al. 2013, Pease et al. 2023).

5. CONCLUSION

Otolith natural markers provided an effective method for studying the life history and population connectivity of *Eleutheronema rhadinum* in the 3 different ecoregions along the coast of China. Our results demonstrated that *E. rhadinum* larvae from different ecoregions had distinct otolith core characteristics, which can be used as discriminative markers for different geographical areas. After the larvae left their nursery grounds, young fish from the colder northern environment migrated southward to overwinter, and mixing occurred in the waters of the SCS continental shelf during foraging and overwintering. After overwintering, they returned to their birthplaces (although the ratio between returnees and those continuing to migrate is unclear), along with adult fish from other sources, leading to a diverse origin of adult fish in each region and a lack of structure. The connectivity of life history stages implied that *E. rhadinum* should be considered as a unit for conservation and management. Its life history is heavily dependent on estuaries and coastal waters, which are greatly affected by human activities (Zhao et al. 2020).

Acknowledgements. We thank the 3 anonymous reviewers for their very detailed and critical comments on this work. This study was supported by a TUYF grant to W.-X.W.

LITERATURE CITED

Alò D, Lacy SN, Castillo A, Samaniego HA, Marquet PA, Tittensor D (2021) The macroecology of fish migration. Glob Ecol Biogeogr 30:99–116

Andrade H, Santos J, Taylor R (2013) Life-history traits of the common snook *Centropomus undecimalis* in a Caribbean estuary and large-scale biogeographic patterns relevant to management. J Fish Biol 82:1951–1974

Aykanat T, Johnston SE, Orell P, Niemela E, Erkinaro J, Primmer CR (2015) Low but significant genetic differentiation underlies biologically meaningful phenotypic divergence in a large Atlantic salmon population. Mol Ecol 24:5158–5174

Baerwald MR, Meek MH, Stephens MR, Nagarajan RP and others (2016) Migration-related phenotypic divergence is associated with epigenetic modifications in rainbow trout. Mol Ecol 25:1785–1800

Baker R, Barnett A, Bradley M, Abrantes K, Sheaves M (2019) Contrasting seascape use by a coastal fish assemblage: a multi-methods approach. Estuaries Coasts 42: 292–307

Benson IM, Kastelle CR, Helser TE, Short JA, Anderl DM (2019) Age interpretation in eulachon (*Thaleichthys pacificus*) as suggested by otolith microchemical signatures. Environ Biol Fishes 102:629–643

Bradley M, Nagelkerken I, Baker R, Sheaves M (2020) Context dependence: a conceptual approach for understanding the habitat relationships of coastal marine fauna. BioScience 70:986–1004

Burns NM, Hopkins CR, Bailey DM, Wright PJ (2020) Otolith chemoscape analysis in whiting links fishing grounds to nursery areas. Commun Biol 3:690

Cao Z, Wang L, Yang L, Yu J, Lv J, Meng M, Li G (2020) Heavy metal pollution and the risk from tidal flat reclamation in coastal areas of Jiangsu, China. Mar Pollut Bull 158:111427

Chen Y, Mao C, Lin N (2015) Influence of abiotic factors on spatiotemporal patterns of larval fish assemblages in the surf zones of the Yangtze River estuary and Hangzhou Bay. J Fish Sci China 22:780–790

Ethier DM, Kyle CJ, Nocera JJ (2014) Tracking animal movement by comparing trace element signatures in claws to spatial variability of elements in soils. Sci Total Environ 468-469:699–705

Fan X, Zhang L, Yuan L, Guo B, Zhang Q, Wang Y, Wu Q (2023) Loss of tidal creek ecosystem vitality caused by tidal flat narrowing on the central Jiangsu coast, China. Sci Total Environ 864:161216

Grammer GL, Morrongiello JR, Izzo C, Hawthorne PJ, Middleton JF, Gillanders BM (2017) Coupling biogeochemical tracers with fish growth reveals physiological and environmental controls on otolith chemistry. Ecol Monogr 87:487–507

Han C, Dong S, Li L, Gao Q (2021) Efficacy of using stable isotopes coupled with chemometrics to differentiate the production method and geographical origin of farmed salmonids. Food Chem 364:130364

Hsieh Y, Shiao JC, Lin SW, Iizuka Y (2019) Quantitative reconstruction of salinity history by otolith oxygen stable isotopes: an example of a euryhaline fish *Lateolabrax japonicus.* Rapid Commun Mass Spectrom 33: 1344–1354

Huang S, He Y (2019) Management of China's capture fisheries: review and prospect. Aquacult Fish 4:173–182

Huang X, Zhao F, Song C, Gao Y, Geng Z, Zhuang P (2017) Effects of stereoscopic artificial floating wetlands on nekton abundance and biomass in the Yangtze Estuary. Chemosphere 183:510–518

Hüssy K, Limburg KE, de Pontual H, Thomas ORB and others (2021) Trace element patterns in otoliths: the role of biomineralization. Rev Fish Sci Aquacult 29:445–477

Itakura H, Arai K, Kaifu K, Shirai K and others (2018) Distribution of wild and stocked Japanese eels in the lower reaches of the Tone River catchment revealed by otolith stable-isotope ratios. J Fish Biol 93:805–813

Izzo C, Reis-Santos P, Gillanders BM (2018) Otolith chemistry does not just reflect environmental conditions: a meta-analytic evaluation. Fish Fish 19:441–454

Jiang T, Liu H, Hu Y, Chen X, Yang J (2022) Revealing population connectivity of the estuarine tapertail anchovy *Coilia nasus* in the Changjiang River estuary and its adjacent waters using otolith microchemistry. Fishes 7:147

Jin B, Fu C, Zhong J, Li B, Chen J, Wu J (2007) Fish utilization of a salt marsh intertidal creek in the Yangtze River estuary, China. Estuar Coast Shelf Sci 73:844–852

Jin B, Qin H, Xu W, Wu J and others (2010) Nekton use of intertidal creek edges in low salinity salt marshes of the Yangtze River estuary along a stream-order gradient. Estuar Coast Shelf Sci 88:419–428

Kawazu M, Tawa A, Ishihara T, Uematsu Y, Sakai S (2020) Discrimination of eastward trans-Pacific migration of the Pacific bluefin tuna *Thunnus orientalis* through otolith $\delta^{13}C$ and $\delta^{18}O$ analyses. Mar Biol 167:110

Killick R, Eckley IA (2014) Changepoint: an R package for changepoint analysis. J Stat Softw 1:1–19

Lin XZ, Ou YJ, Li JE, Wen JF, Wang PF (2015) Present status and foreground of family threadfin fishes (Polynemidae). J Biol 32:83–87 (in Chinese with English abstract)

Lowerre-Barbieri SK, Walters Burnsed SL, Bickford JW (2016) Assessing reproductive behavior important to fisheries management: a case study with red drum, *Sciaenops ocellatus.* Ecol Appl 26:979–995

Mao C, Zhong J, Fang Y, Ge C, Yang P, Chen Y, Chen X (2013) Species composition and habitat use patterns of fish larvae and juveniles inhabiting the surf zone of a sandy beach at Sijiao Island. J Fish Sci China 20:166–176

Martín-Vélez V, Mohring B, van Leeuwen CHA, Shamoun-Baranes J and others (2020) Functional connectivity network between terrestrial and aquatic habitats by a generalist waterbird, and implications for biovectoring. Sci Total Environ 705:135886

Matta ME, Miller JA, Short JA, Helser TE, Hurst TP, Rand KM, Ormseth OA (2019) Spatial and temporal variation in otolith elemental signatures of age-0 Pacific cod (*Gadus macrocephalus*) in the Gulf of Alaska. Deep Sea Res II 165:268–279

McCulloch M, Cappo M, Aumend J, Müller W (2005) Tracing the life history of individual barramundi using laser ablation MC-ICP-MS Sr-isotopic and Sr/Ba ratios in otoliths. Mar Freshw Res 56:637–644

McDowall RM (1997) The evolution of diadromy in fishes (revisited) and its place in phylogenetic analysis. Rev Fish Biol Fish 7:443–462

Menezes R, Moura PE, Santos AC, Moraes LE, Condini MV, Rosa RS, Albuquerque CQ (2021) Habitat use plasticity by the dog snapper (*Lutjanus jocu*) across the Abrolhos Bank shelf, eastern Brazil, inferred from otolith chemistry. Estuar Coast Shelf Sci 263:107637

Micheletti SJ, Matala AR, Matala AP, Narum SR (2018) Landscape features along migratory routes influence adaptive genomic variation in anadromous steelhead (*Oncorhynchus mykiss*). Mol Ecol 27:128–145

Millar RB (1987) Maximum likelihood estimation of mixed stock fishery composition. Can J Fish Aquat Sci 44: 583–590

Millar RB (1990) Comparison of methods for estimating mixed stock fishery composition. Can J Fish Aquat Sci 47:2235–2241

Mischel SA, Mertz-Kraus R, Jochum KP, Scholz D (2017) TERMITE: an R script for fast reduction of laser ablation inductively coupled plasma mass spectrometry data and its application to trace element measurements. Rapid Commun Mass Spectrom 31:1079–1087

Morissette O, Sirois P (2021) Flowing down the river: influence of hydrology on scale and accuracy of elemental composition classification in a large fluvial ecosystem. Sci Total Environ 760:143320

Motomura H (2004) Threadfins of the world (family Polynemidae). An annotated and illustrated catalogue of polynemid species known to date. FAO, Rome

Muto D, Ishimura T, Takahashi M, Nishida K (2022) Extracting daily isotopic records on fish otolith (*Trachurus japonicus*) by combining micro-milling and micro-scale isotopic analysis (MICAL-CF-IRMS). Rapid Commun Mass Spectrom 36:e9366

Patra S, Liu CQ, Wang FS, Li SL, Wang BL (2012) Behavior of major and minor elements in a temperate river estuary to the coastal sea. Int J Environ Sci Technol 9:647–654

Pease AA, Jacobs GR, Mendoza-Carranza M, Rodiles-Hernández R, Wenger SJ, Capps KA (2023) Otolith microchemistry highlights the importance of extensive connectivity for conservation of an iconic migratory fish in a large tropical river basin. Aquat Conserv 33:969–980

Quan W, Zhu J, Ni Y, Shi L, Chen Y (2009a) Faunal utilization of constructed intertidal oyster (*Crassostrea rivularis*) reef in the Yangtze River estuary, China. Ecol Eng 35:1466–1475

Quan W, Ni Y, Shi L, Chen Y (2009b) Composition of fish communities in an intertidal salt marsh creek in the Changjiang River estuary, China. Chin J Oceanol Limnol 27:806–815

Reis-Santos P, Gillanders BM, Tanner SE, Vasconcelos RP, Elsdon TS, Cabral HN (2012) Temporal variability in estuarine fish otolith elemental fingerprints: implications for connectivity assessments. Estuar Coast Shelf Sci 112: 216–224

Russell A, Taylor MD, Barnes TC, Johnson DD, Gillanders BM (2022) Habitat transitions by a large coastal sciaenid across life history stages, resolved using otolith chemistry. Mar Environ Res 176:105614

Sakamoto T, Takahashi M, Chung MT, Rykaczewski RR and others (2022) Contrasting life-history responses to climate variability in eastern and western North Pacific sardine populations. Nat Commun 13:5298

Sharma A, Paliwal KK (2015) Linear discriminant analysis for the small sample size problem: an overview. Int J Mach Learn Cybern 6:443–454

Shihab I, Gopalakrishnan A, Vineesh N, Muktha M, Akhilesh KV, Vijayagopal P (2017) Histological profiling of gonads depicting protandrous hermaphroditism in *Eleutheronema tetradactylum.* J Fish Biol 90:2402–2411

Smoliński S, Schade FM, Berg F (2020) Assessing the performance of statistical classifiers to discriminate fish stocks using Fourier analysis of otolith shape. Can J Fish Aquat Sci 77:674–683

Sturrock AM, Hunter E, Milton JA, Johnson RC, Waring CP, Trueman CN, Leder E (2015) Quantifying physiological influences on otolith microchemistry. Methods Ecol Evol 6:806–816

Su NJ, Lu YS, Wang CH, Liao CH, Chiang WC, Tseng CT (2020) Age determination for juvenile fourfinger threadfin (*Eleutheronema rhadinum*) by using otolith microstructure and length data obtained from commercial fisheries off northwestern Taiwan. Fish Res 227: 105560

Sun X, Xu D, Lou B, Zhang T, Xin J, Guo Y, Ma S (2013) Genetic diversity and population structure of *Eleutheronema rhadinum* in the East and South China Seas revealed in mitochondrial COI sequences. Chin J Oceanol Limnol 31:1276–1283

Thomas OR, Ganio K, Roberts BR, Swearer SE (2017) Trace element–protein interactions in endolymph from the inner ear of fish: implications for environmental reconstructions using fish otolith chemistry. Metallomics 9: 239–249

Wang X, Xiao X, Zou Z, Chen B and others (2020) Tracking annual changes of coastal tidal flats in China during 1986–2016 through analyses of Landsat images with Google Earth Engine. Remote Sens Environ 238:110987

Whitfield AK (2020) Littoral habitats as major nursery areas for fish species in estuaries: a reinforcement of the reduced predation paradigm. Mar Ecol Prog Ser 649: 219–234

Xuan Z, Wang WX (2023) Diversity of life history and population connectivity of threadfin fish *Eleutheronema tetradactylum* along the coastal waters of Southern China. Sci Rep 13:3976

Xuan Z, Wang X, Hajisamae S, Tsim KWK, Yang J, Wang WX (2022) Otolith microchemistry reveals different environmental histories for two endangered fourfinger threadfin species. Mar Ecol Prog Ser 700:161–178

Ye X, Liu J, Lin M, Ding J, Zou B, Song Q (2021) Global ocean chlorophyll-*a* concentrations derived from COCTS onboard the HY-1C satellite and their preliminary evaluation. IEEE Trans Geosci Remote Sens 59:9914–9926

Younes AF, Cerrato RM, Nye JA (2020) Overwintering survivorship and growth of young-of-the-year black sea bass *Centropristis striata*. PLOS ONE 15:e0236705

Zhang Y, Huang G, Wang W, Chen L, Lin G (2012) Interactions between mangroves and exotic *Spartina* in an anthropogenically disturbed estuary in southern China. Ecology 93:588–597

Zhao C, Qin CZ, Teng J (2020) Mapping large-area tidal flats without the dependence on tidal elevations: a case study of Southern China. ISPRS J Photogramm Remote Sens 159:256–270

Zheng Q, Fang G, Song YT (2006) Introduction to special section: Dynamics and circulation of the Yellow, East, and South China Seas. J Geophys Res 111:C11S01

Editorial responsibility: Stephen Wing, Dunedin, New Zealand
Reviewed by: R. Francini Filho and 2 anonymous referees

Submitted: May 1, 2023
Accepted: January 12, 2024
Proofs received from author(s): February 29, 2024